

All You Need is an Improving Column: Enhancing Column Generation for Parallel Machine Scheduling via Transformers

Amira Hijazi

NSF AI Institute for Advances in Optimization (AI4OPT),
Georgia Institute of Technology, Atlanta, GA

Osman Ozaltin, Reha Uzsoy

Edward P. Fitts Department of Industrial and Systems Engineering,
North Carolina State University

Abstract

We present a neural network-enhanced column generation (CG) approach for a parallel machine scheduling problem. The proposed approach utilizes an encoder-decoder attention model, namely the transformer and pointer architectures, to develop job sequences with negative reduced cost and thus generate columns to add to the master problem. By training the neural network offline and using it in inference mode to predict negative reduced costs columns, we achieve significant computational time savings compared to dynamic programming (DP). Since the exact DP procedure is used to verify that no further columns with negative reduced cost can be identified at termination, the optimality guarantee of the original CG procedure is preserved. For small to medium-sized instances, our approach achieves an average 45% reduction in computation time compared to solving the subproblems with DP. Furthermore, the model generalizes not only to unseen, larger problem instances from the same probability distribution but also to instances from different probability distributions than those presented at training time. For large-sized instances, the proposed approach achieves an 80% improvement in the objective value in under 500 seconds, demonstrating both its scalability and efficiency.

Keywords: *Column Generation, Machine Learning, Transformers, Parallel Machine Scheduling*

1 Introduction

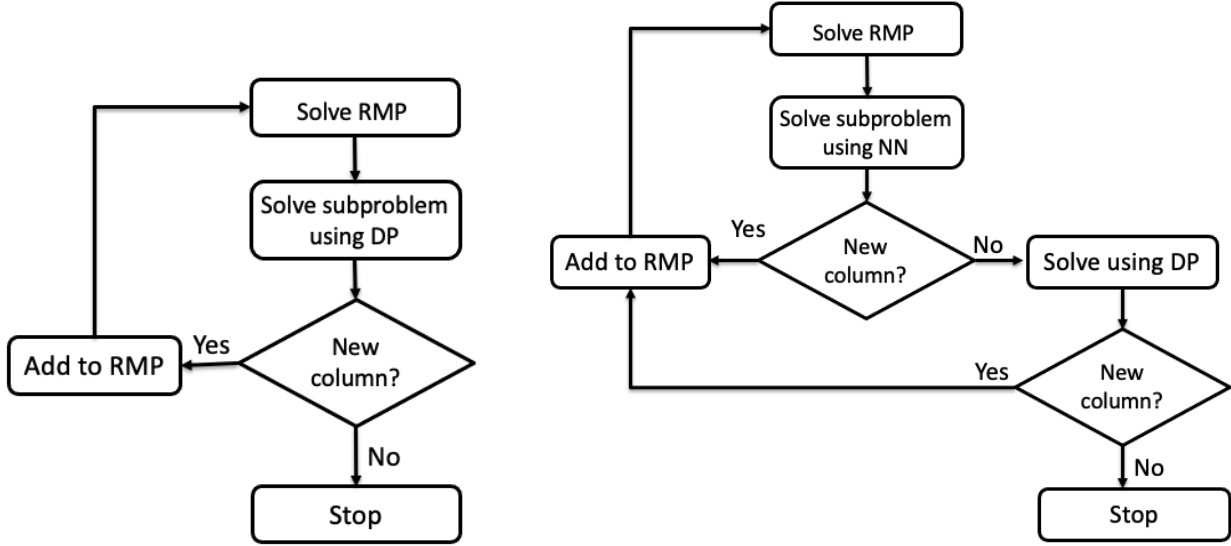
Parallel machine scheduling has applications in many manufacturing and service systems (Weng et al., 2001; Hall et al., 2000; Baesler and Palma, 2014). The problem involves allocating and sequencing a set of jobs $N = \{1, 2, \dots, n\}$ on a set of parallel machines $M = \{1, 2, \dots, m\}$ where each job is assigned to only one machine and each machine can process only one job at a time. An instance of the parallel machine scheduling problem is defined by the job attributes (processing time, weight), machine environment (identical, proportional, or unrelated), and a performance measure such as makespan (Mokotoff, 2001), total weighted completion time (Chen and Powell, 1999), or total tardiness (Yalaoui and Chu, 2002). We consider the problem of minimizing the total weighted completion time on unrelated parallel machines (Lawler et al., 1993). In this problem, each job $j \in N$ has a weight w_j and a processing time p_{jk} on machine $k \in M$. The job processing times on different machines are independent of each other, hence *unrelated* machines.

A common solution approach for this problem is column generation (Wilhelm, 2001; Lübbecke and Desrosiers, 2005). Each iteration of column generation involves solving a linear program, called the restricted master problem (RMP), restricted to a subset of the variables. Additional columns that will improve the objective function value of the RMP are generated as needed by solving an application-specific pricing subproblem. If such columns are found, they are added to the restricted LP, which is re-optimized. Iterations continue until no further improving columns can be found. The optimal solution of the restricted master problem must then be processed in some way to obtain a feasible integer solution. The pricing subproblem for the scheduling problem we consider is a single-machine scheduling problem that can be solved using a pseudo-polynomial time dynamic programming (DP) algorithm, which becomes computationally expensive as the instance size increases.

In this paper, we leverage the capabilities of machine learning (ML), specifically neural networks, to rapidly approximate the solution of the pricing subproblem to obtain improving columns with negative reduced cost. Flowcharts of the traditional CG approach with DP (CG-DP) and our proposed CG approach (CG-NN-DP) are illustrated in Figure 1. In our proposed approach, if the column generated by the NN has a negative reduced cost, we add it to the RMP and reoptimize. If no column with a negative reduced cost is predicted by the NN, we solve the subproblem using DP to confirm that no further improving columns exist. Since the neural network is trained offline and used in inference mode to predict a job sequence with a negative reduced cost, the savings in computation time over the DP are significant. Since the exact DP procedure is used to verify that no further columns with negative reduced cost can be identified at termination, the optimality guarantee of the original CG procedure is preserved. The proposed neural network uses the transformer architecture with a pointer layer. Transformers are encoder-decoder attention-based neural networks designed for sequential data tasks that have been successfully used in language translation and generating graph structures (Yun et al., 2020). In the combinatorial optimization domain, transformers have been used for solving the Traveling Salesman Problem (TSP) (Kool et al., 2018), Vehicle Routing Problem (Wu et al., 2024), Knapsack Problem (Lee et al., 2024), and Job Shop Scheduling (Yildiz, 2022). The main advantages of transformers over Recurrent Neural Networks (RNN) and Long Short-Term Memory Networks (LSTM) networks arise from enhanced modeling of the interactions between the different input vectors representing job and machine parameters and improved training efficiency due to the attention mechanism.

Our initial experiments using a transformer architecture alone were only able to achieve 45% validation accuracy and failed to generate negative reduced cost columns when used within the CG in the testing phase, so we added a pointer layer to the transformer to improve the learning. Pointer networks were

Figure 1: CG-DP vs CG-NN-DP



introduced by Vinyals et al. (2015) based on sequence-to-sequence networks (Sutskever et al., 2014) to learn the conditional probability $p(C^P|P)$ of an output sequence C^P with elements corresponding to positions in an input set P . They have been used successfully in approximating solutions to several combinatorial optimization problems, such as finding the convex hull and Delaunay triangulation (Vinyals et al., 2015), the Traveling Salesman Problem (Stohy et al., 2021; Ma et al., 2019), and the selection of branching variables in branch and bound algorithms (Wang et al., 2024). Pointer networks have demonstrated their ability to generalize to instances larger than those in the training sets, making them well-suited for combinatorial optimization problems like parallel machine scheduling.

1.1 Literature Review

Parallel Machine Scheduling. Most variants of the parallel machine scheduling problem, including that addressed in this paper, are NP-hard in the strong sense, rendering them computationally challenging for commercial solvers (Pfund et al., 2004; Li and Yang, 2009). A variety of exact and approximation solution methods have been developed as a result. Phillips et al. (1994) proposed the first polynomial-time approximation algorithm for minimizing the total weighted completion time on unrelated parallel machines. Azizoglu and Kirca (1999) developed an exact branch and bound algorithm capable of solving small instances (up to three machines and 20 jobs). Chen and Powell (1999) developed a branch and price algorithm, which forms the basis of the approach in this paper. The extensive literature on parallel machine scheduling problems is reviewed by Mokotoff (2001); Li and Yang (2009) and Durasević and Jakobović (2023).

ML for Combinatorial Optimization. Machine learning techniques have been applied to combinatorial optimization problems through two distinct strategies. The first involves using ML tools to enhance decision-making within optimization algorithms themselves, either through supervised learning or reinforcement learning. Khalil et al. (2016) proposed a supervised learning framework for variable branching in mixed integer programming imitating the strong branching rule. Tang et al. (2020) utilized a reinforcement learning framework to learn a cut selection policy for the cutting plane algorithm, which is used in branch-and-cut

solvers. [Rajabalizadeh and Davarnia \(2024\)](#) used classification techniques to approximate the optimal value of cut-generating linear programs. The second strategy involves using ML tools to approximate solutions to difficult optimization problems, often referred to as "optimization proxies." [Bresson and Laurent \(2021\)](#) trained a reinforcement learning agent to solve the TSP problem for instances as large as 100 nodes while [Hertrich and Skutella \(2023\)](#) developed an RNN to predict solutions to the knapsack problem. [Ojha et al. \(2023\)](#) developed an optimization proxy for outbound load planning in the parcel service industry using supervised learning. We refer the readers to survey papers by [Bengio et al. \(2021\)](#); [Mazyavkina et al. \(2021\)](#); [Kotary et al. \(2021\)](#); [Zhang et al. \(2023\)](#); [Cappart et al. \(2023\)](#), and [Fan et al. \(2024\)](#).

ML for Column Generation. Several recent studies have applied ML methods to Column Generation. [Sugishita et al. \(2024\)](#) utilized ML to generate initial dual values to warm-start the column generation procedure for unit commitment problem. [Morabit et al. \(2021\)](#) proposed a supervised Graph Neural Network (GNN) approach for selecting the most promising column from a set of available columns obtained by solving the pricing problem. They demonstrate the effectiveness of their approach on the Vehicle and Crew Scheduling Problem and the Vehicle Routing Problem with Time Windows, obtaining reductions in computing time of up to 30%.

Instead of relying on a time-consuming exact method, [Chi et al. \(2022\)](#) adopt deep reinforcement learning with GNN to optimize the column selection based on the maximum expected future reward. Their experimental results demonstrate significant reductions in the number of column generation (CG) iterations for the Vehicle Routing Problem with Time Windows compared to the traditional greedy column selection policy. In contrast, [Shen et al. \(2022\)](#) used supervised machine learning techniques to construct a pricing heuristic for the graph coloring problem. A linear Support Vector Machine is used to predict the optimal solution for the pricing problem, which is then used to guide an efficient sampling technique that generates many high-quality columns. The findings indicate a significant decrease in the number of pricing iterations needed, resulting in faster convergence and enhanced computational efficiency.

1.2 Contributions and Organization

In this paper, we train a neural network (NN) to speed up the CG solution time by predicting the optimal solution to the pricing subproblem instead of relying solely on dynamic programming. The contributions of this paper are as follows:

1. We propose a ML approach to predict the optimal solution of a difficult combinatorial scheduling problem, namely the single machine scheduling subproblem.
2. The proposed approach is integrated with the CG approach to obtain a new column for each pricing subproblem by predicting a candidate sequence of jobs for the associated machine instead of using DP. If no column with a negative reduced cost is predicted by the neural network, we solve the subproblem using dynamic programming to confirm that no further improving columns exist. This approach achieves significant time reduction and improved convergence compared to the greedy CG with DP, while preserving the optimality guarantee of the original CG procedure.
3. We train a single model that considers different instance sizes, including different numbers of machines and jobs, and demonstrate its ability to generalize performance beyond the instance sizes and parameter distributions in the training set.

Section 2 presents the parallel machine scheduling problem formulation, and Section 3 introduces the different solution methods. Section 4 includes details about the data generation pipeline and Section 5 describes the experiment settings. Section 6 reports the computational results, and Section 7 concludes the paper.

2 Problem Formulation

We consider the problem of minimizing the total weighted completion time on unrelated parallel machines, denoted by $R||\sum w_j C_j$ in the standard three-field notation (Pinedo, 2012), where C_j denotes the completion time of job j in a schedule and w_j the weight of job j . The objective is to assign jobs to machines and sequence the assigned jobs on each machine to minimize the total weighted completion time. All jobs are simultaneously available with no precedence constraints or setup times. Our point of departure is the branch and price approach of Chen and Powell (1999), who use Dantzig-Wolfe decomposition (Dantzig and Wolfe, 1960) to decompose their original integer programming formulation into a set partitioning master problem and pricing subproblems associated with each of the machines that are solved using dynamic programming.

Let M denote the set of machines and Ω_k the set of all possible schedules on machine k in which a subset of jobs is processed on that machine. For a schedule s_k containing l jobs, the job sequence must follow the shortest weighted processing time (SWPT) order (Smith et al., 1956); $\frac{p_{[1]}}{w_{[1]}} \leq \frac{p_{[2]}}{w_{[2]}} \leq \dots \leq \frac{p_{[l]}}{w_{[l]}}$ where $[i]$ denotes the job j with the i th smallest value of $\frac{p_j}{w_j}$. The total weighted completion time of schedule s_k on machine k is given by $f_s^k = \sum_{i=1}^l w_{[i]} C_{[i]}$.

For each job $j \in N$, let $a_{j_s}^k = 1$ if job j is processed in schedule $s_k \in \Omega_k$ on machine k , and 0 otherwise. Defining the 0-1 decision variables y_s^k for $k \in M, s \in \Omega^k$ as:

$$y_s^k = \begin{cases} 1, & \text{if schedule } s \in \Omega^k \text{ is used} \\ 0, & \text{otherwise} \end{cases}$$

the set partitioning master problem proposed in Chen and Powell (1999) is written as :

$$(MP) \quad \min \sum_{k \in M} \sum_{s \in \Omega^k} f_s^k y_s^k \tag{1}$$

$$\sum_{k \in M} \sum_{s \in \Omega^k} a_{j_s}^k y_s^k = 1 \quad \forall j \in N \quad (\pi_j) \tag{2}$$

$$\sum_{s \in \Omega^k} y_s^k \leq 1 \quad \forall k \in M \quad (\sigma_k) \tag{3}$$

$$y_s^k \in \{0, 1\} \quad \forall s \in \Omega^k, k \in M \tag{4}$$

The objective function (1) minimizes $\sum w_j C_j$ over all machines. Constraints (2) ensure that each job is processed in exactly one partial schedule, and (3) that at most one schedule is selected for each machine. The LP relaxation of the master problem is obtained by relaxing constraints (4) such that $0 \leq y_s^k \leq 1$. Constraints (3) satisfy the upper bound constraints $y_s^k \leq 1$, making explicit upper bound constraints redundant.

The **column generation** approach starts by solving an LP relaxation of the MP with a restricted number of columns, the Restricted Master Problem (RMP), where a column represents a feasible schedule for a given machine. A single machine subproblem for each machine $k \in M$ is solved using dynamic programming to

find a feasible schedule $s \in \Omega^k$ with negative reduced cost. The reduced cost of a feasible schedule $s \in \Omega^k$ on machine $k \in M$ is given by:

$$r_s^k = f_s^k - \sum_{j \in N} a_{js}^k \pi_j - \sigma_k, \quad (5)$$

where π_j , $j \in N$ denote the dual variables associated with constraints (2) and σ_k , $k \in K$ those associated with constraints (3).

If such columns exist, they enter the basis, and the LP relaxation of the RMP is re-optimized until no such columns can be found. If the optimal solution at this point satisfies the integrality property, then the solution is optimal for the original IP problem. However, this is generally not the case. Therefore, column generation is combined with branch and bound to find integer solutions, and this method is called branch and price. In this work, we restrict our focus on column generation. For small to medium-sized instances, we run the CG until no further columns with a negative reduced cost can be found and then solve the restricted master problem containing all columns present in the final solution to its LP relaxation with integer y_s^k , to ensure we have an integer solution, thus obtaining an optimality certificate of the original integer program. For large instances, we run the CG with a time limit so optimality is not guaranteed.

Initial Solution. A feasible solution to the RMP is required to initiate the column generation procedure. For this purpose, we explore two different list scheduling heuristics. The first randomly selects a subset of jobs, with each job having an equal likelihood of being chosen, and sorts them based on the SWPT rule. The number of times the heuristic is executed per machine ranges from 5 to 100, depending on the instance size. The second heuristic generates a random permutation of the jobs and sequentially assigns each job to the machine with the minimum total weighted completion time. The heuristic is executed 2,000 times to generate a diverse set of initial solutions. The 20 solutions with the lowest total weighted completion times are selected to initiate the column generation procedure. Despite its potential advantages, we did not observe any significant time improvement overall when using the second heuristic. Therefore, we employ the computationally more efficient first heuristic to initialize the column generation (CG) instances used for training and testing the neural network.

3 Pricing Subproblem Solution Methods

In this section, we present the dynamic programming approach for the subproblems and the neural network approaches: a transformer neural network and a transformer pointer neural network.

3.1 Baseline Solution Method: Dynamic Programming

The pseudo-polynomial time dynamic programming algorithm in [Chen and Powell \(1999\)](#) derives from the procedure by [Rothkopf \(1966\)](#), which exploits the fact that in any optimal schedule for the $R||\sum w_j C_j$ problem, jobs on each machine must follow the SWPT sequence. Their algorithm for the pricing subproblem, stated in [Algorithm 1](#), defines the recursion function $F(j, t)$ as the minimum objective function value of a schedule containing a subset of jobs $\{1, 2, \dots, j\}$ sequenced by the SWPT rule and completed at time t . The pseudo-polynomial time complexity of this DP is due to its selecting a subset of jobs for the partial schedule, rendering it NP-hard in the ordinary sense ([Garey and Johnson, 1979](#)). The worst-case time complexity of this algorithm is $O(n^2P)$, where P denotes the total processing time of all jobs and n the number of jobs, which can be computationally expensive for large instances with long processing times, motivates our proposal to replace the DP with a machine learning model.

Algorithm 1: Chen et al. Dynamic Programming Algorithm

Initialize: $F(j, t) = \infty, t < 0, j = 0, \dots, n$
 $F(0, t) = 0, t \geq 0$
for $j \in (1, \dots, n)$ **do**
 for $t \in (0, \dots, P)$ **do**
 $F(j, t) = \min\{F(j-1, t-p_j) + tw_j - \pi_j, F(j-1, t)\}$
 end
end
Return : $\min_{j \in N, 0 \leq t \leq P} \{F(j, t)\}$

3.2 Neural Network Approaches

In the NN framework, an instance (X, s) of the pricing subproblem corresponds to a single machine scheduling subproblem encountered in one CG iteration on a specific machine m , where s is the target schedule for input feature matrix $X = [x_0, x_1, \dots, x_n]$. The first row of the input matrix X is the machine vector: $x_0 = [0, 0, \sigma_m]$, where σ_m is the dual variable associated with machine m via constraints (3). Each job is represented by a row $x_j = [p_{jm}, w_j, \pi_j]$, where the job features p_{jm}, w_j, π_j denote its processing time on machine m , weight, and the value of its associated dual variable via constraints (2) in the current solution to the restricted master problem, respectively. The target schedule s consists of a subset of jobs on machine m in SWPT sequence yielding the most negative reduced cost computed by the dynamic program.

To predict s given input X , we utilize a NN model with learnable weights θ . The NN model estimates the probability $p_m(s|X; \theta)$ based on the chain rule:

$$p_m(s|X; \theta) = \prod_{i=1}^n p_m(s_i | s_0, \dots, s_{i-1}, X; \theta)$$

The conditional probability $p_m(s_i | s_0, \dots, s_{i-1}, X; \theta)$ indicates the likelihood of selecting s_i to be in the i th schedule position, given the input X and previously selected elements s_0, \dots, s_{i-1} in the schedule. The predicted schedule \hat{s} is chosen to be the one with the highest probability, i.e., $\hat{s} \in \arg \max p(s|X; \theta)$.

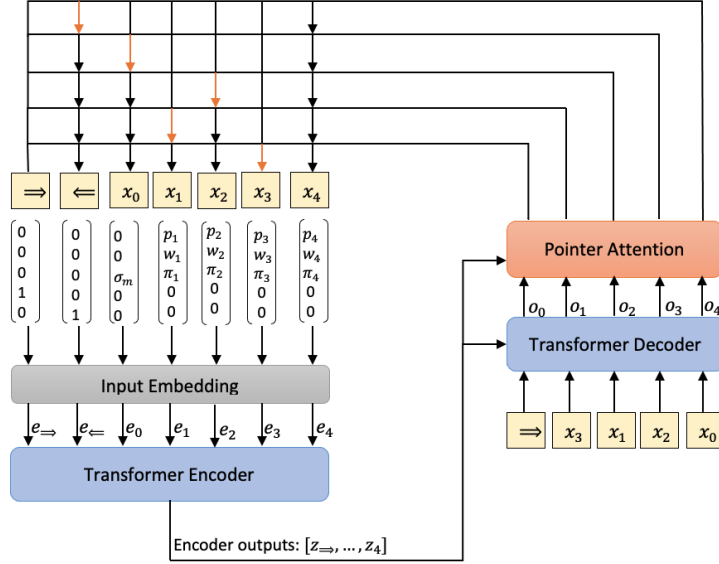
3.2.1 Input Preprocessing

To prepare the input X for the transformer architecture, we append two special vectors to it indicating the start, denoted by (\Rightarrow) , and end of the schedule, denoted by (\Leftarrow) . \Rightarrow is represented by the 1×5 vector $[0, 0, 0, 1, 0]$ and \Leftarrow by $[0, 0, 0, 0, 1]$. The job input vector x_j and machine input vector x_0 are then modified as: $x_j = [p_{jm}, w_j, \pi_j, 0, 0]$ and $x_0 = [0, 0, \sigma_m, 0, 0]$ to ensure consistent dimensions for matrix operations, padding and masking, batch processing, and parallel computation.

The target schedule is also preprocessed to include the machine, \Rightarrow , and \Leftarrow elements. For example, target schedule $[3, 1, 2]$ is input to the network as $s = [\Rightarrow, 3, 1, 2, 0, \Leftarrow]$ where \Rightarrow (s_0) indicates the beginning of the schedule, $s_1 = 3, s_2 = 1, s_3 = 2$ the indices of the job vectors, and 0 the index of the machine vector in the input sequence. Although we use the machine vector index 0 after the last job index in the schedule, we still need \Leftarrow to indicate the end of schedule because the machine vector differs between different input instances while \Leftarrow remains constant. Henceforth we refer to s as a schedule and NN output interchangeably.

Figure 2 illustrates the proposed neural network architecture for an example single machine scheduling subproblem with 4 jobs. In this example, the input matrix $X \in R^{7 \times 5}$ involves 7 elements: \Rightarrow , \Leftarrow , machine, and four jobs, each of which is represented by a 1×5 vector. We first pass X through an embedding layer that projects each input vector to a d dimensional space, where d is a hyperparameter (set to 64

Figure 2: Transformer-Pointer Network with input $X = \{x_0, x_1, x_2, x_3, x_4\}$, and output $\{\Rightarrow, 3, 1, 2, 0, \Leftarrow\}$ from which we have the output schedule $[3, 1, 2]$. The elements \Rightarrow and \Leftarrow represent the beginning and end of the schedule, respectively and 0 the machine elements. Note that job 4 represented by x_4 is not selected in the partial schedule.



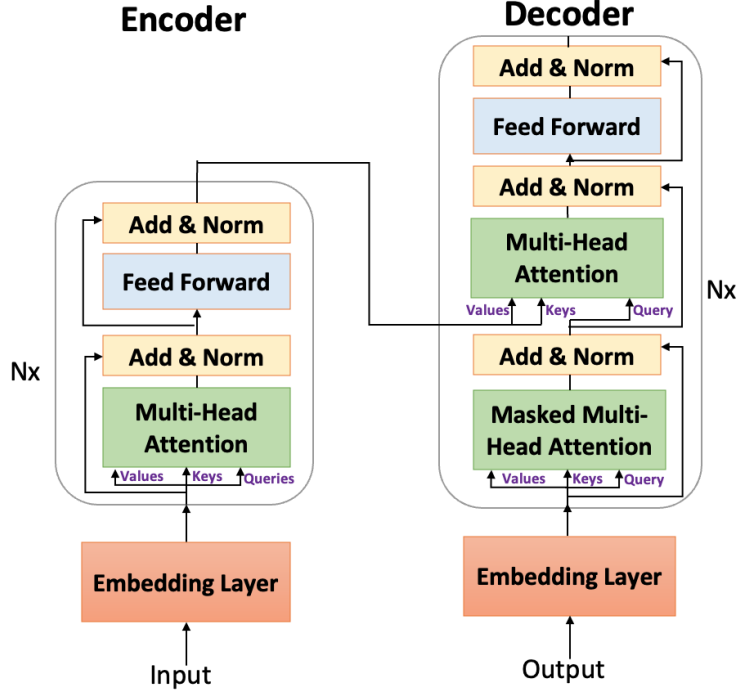
through hyperparameter tuning described in Section 5.2). The matrix operation in the embedding layer is $E = XW_{\text{embed}}$, where $W_{\text{embed}} \in R^{5 \times d}$ is a weight matrix learned by training. Each row e_i of E represents the embedding corresponding to input x_i . The embedding layer facilitates the training of the model by providing smooth, continuous input to the network. The total number of learnable parameters in the embedding layer is given by the number of elements in $W_{\text{embed}} \in R^{5 \times d}$. In our case, with 5 input features and $d = 64$, $5 \times 64 = 320$ weights are trained for this portion of the architecture.

3.2.2 Transformer Network

We employ the transformer architecture (Vaswani et al., 2017) depicted in Figure 3 as a baseline. A transformer consists of an encoder and a decoder, both of which utilize the *multi-head attention mechanism*, which plays a crucial role in capturing dependencies within an input sequence, essential for modeling interactions between jobs and the machine in our pricing subproblem.

Attention Mechanism. The attention mechanism was introduced to improve the performance of neural networks in tasks involving long sequences, such as machine translation. In its most general form, the attention mechanism computes a weighted sum of *values* corresponding to elements in the input sequence. The weights are determined by the similarity (often through dot-product or other scoring functions) between a set of *queries* and *keys*, where the queries search for the information that a model is looking for, and the keys represent various characteristics of the input elements. If keys, queries, and values are derived from the same input sequence, the mechanism is referred to as *self-attention* and allows tokens of the sequence to attend to each other. Mathematically, given an embedding matrix $E \in R^{n \times d}$ for an input sequence with n tokens, let $Q = EW^Q + \mathbf{1}_n b^Q$, $K = EW^K + \mathbf{1}_n b^K$ and $V = EW^V + \mathbf{1}_n b^V$ for column vector of ones $\mathbf{1}_n \in R^{n \times 1}$, weight matrices $W^Q \in R^{d \times d_k}$, $W^K \in R^{d \times d_k}$, $W^V \in R^{d \times d_v}$, and bias vectors $b^Q, b^K \in R^{1 \times d_k}$, $b^V \in R^{1 \times d_v}$. The resulting $Q \in R^{n \times d_k}$, $K \in R^{n \times d_k}$ and $V \in R^{n \times d_v}$ matrices are referred to as the *query*,

Figure 3: Transformer-based Encoder and Decoder. Figure adapted from Vaswani et al. (2017) where N is the number of layers.



key, and *value* matrices, respectively. The attention score is then computed as:

$$\text{Attention}(Q, K, V) = \text{softmax}\left(\frac{QK^T}{\sqrt{d_k}}\right)V. \quad (6)$$

The softmax operation normalizes the weights in each column of the attention matrix between 0 and 1 in such a way that they add up to 1. The final matrix obtained from the attention mechanism is in $R^{n \times d_v}$ and captures the relation between each pair of tokens in the input sequence.

Masked Attention During training, the entire target sequence is available, and all sequence positions are generated (decoded) in parallel. Therefore, in the decoder part of the transformer, a masked version of self-attention is used to ensure that only tokens decoded in the earlier steps s_0, s_1, \dots, s_{t-1} but not future tokens are considered when decoding the next token s_t . For a target schedule of length n , the mask takes the form of an $n \times n$ upper triangular matrix M given by:

$$M_{ij} = \begin{cases} 0 & \text{if } j \leq i \\ -\infty & \text{if } j > i \end{cases}$$

The masked attention mechanism is then computed by:

$$\text{Attention}(Q, K, V) = \text{softmax}\left(\frac{QK^T}{\sqrt{d_k}} + M\right)V. \quad (7)$$

This mask fills the attention score for the positions of future tokens with negative infinity. Masking is also required during inference because the model's self-attention is inherently parallel and operates over all

positions in the sequence, even when future tokens have not yet been generated. The mask prevents the model from mistakenly trying to attend to future positions, ensuring that each token is generated autoregressively based only on previously generated tokens.

Multi-Head Attention. The transformer utilizes a multi-head attention mechanism by deriving multiple query, key, and value matrices, each with its own set of weight matrices. The self-attention is then applied to these representations in parallel. The outputs of the attention heads are concatenated and linearly projected to generate the final output. In particular,

$$\text{MultiHead}(Q, K, V) = \text{Concat}(\text{head}_1, \dots, \text{head}_h)W^O + \mathbf{1}_n b^O \quad (8)$$

where $\text{head}_i = \text{Attention}(Q_i, K_i, V_i) \in R^{n \times d_v}$ for $i = 1, \dots, h$, the outer projection matrix $W^O \in R^{hd_v \times d}$ and bias vector $b^O \in R^{1 \times d}$. We use $d_k = d_v = \frac{d}{h}$ where the number of heads $h = 8$ and hidden dimension $d = 64$. Thus, for each head i , we have $W_i^Q \in R^{64 \times 8}$ with $b_i^Q \in R^{1 \times 8}$, $W_i^K \in R^{64 \times 8}$ with $b_i^K \in R^{1 \times 8}$, and $W_i^V \in R^{64 \times 8}$ with $b_i^V \in R^{1 \times 8}$ and there are $3 \times (64 \times 8 + 8) = 1,560$ learnable weights per head. Furthermore, the outer projection matrix $W^O \in R^{64 \times 64}$ with $b^O \in R^{1 \times 64}$. Thus, the total number of learnable parameters for the multi-head attention mechanism with 8 heads is $8 \times 1,560 + 64 \times 64 + 64 = 16,640$.

Transformer Encoder. The transformer encoder stacks N sequential layers, each of which comprises two sub-layers: a multi-head self-attention sublayer and a fully connected feed-forward network, as shown in Figure 3. The output of the multi-head self-attention is passed through a feed-forward network. In the first encoder layer, Q, K, V matrices are derived from the input embedding E . In the subsequent encoder layers, these matrices are derived from the output of the previous layer. The output of the encoder is denoted by a context matrix $Z \in R^{n \times d}$. Each row of the context matrix corresponds to a specific token of the input sequence and captures the interactions between that token and all others in the same sequence. Layer normalization is applied after each sublayer through $\text{LayerNorm}(g + \text{Sublayer}(g))$, where $\text{Sublayer}(g) \in R^d$ is the output of the sublayer (e.g. multi-head self-attention) and $g \in R^d$ is the input to the sublayer (e.g. embedding for each input token). Let $\varrho = g + \text{Sublayer}(g)$, $\mu = \sum_{i=1}^d \varrho_i / d$ and $\sigma = \sqrt{\frac{1}{d} \sum_{i=1}^d (\varrho_i - \mu)^2}$ then

$$\text{LayerNorm}(\varrho) = \frac{\varrho - \mu}{\sigma} \odot w_L + b_L,$$

where \odot represents element-wise multiplication, and $w_L \in R^d$ and $b_L \in R^d$ are learnable normalization weight and bias vectors. Thus, for $d = 64$, each layer normalization has a total of 128 learnable parameters. In the transformer architecture, layer normalization helps reduce internal covariate shift and ensures that the input distribution remains consistent as it passes through the layers, enabling more stable training and faster convergence. Since layer normalization operates independently on each token, it is well-suited for sequence models where input sizes or sequences may vary (Ba et al., 2016).

The feed-forward sublayer consists of two linear layers, each with a $d \times d$ weight matrix and a bias vector $\in R^d$. Thus, for $d = 64$, the total number of learnable parameters in the feed-forward sublayer is $2 \times (64 \times 64 + 64) = 8,320$. The number of learnable parameters per encoder layer is the total number of weights for the multi-head self-attention sublayer, feed-forward sublayer, and two layer normalization which is: $16,640 + 8,320 + 2 \times 128 = 25,216$. For $N = 2$ encoder layers, the total number of encoder parameters is $2 \times 25,216 = 50,432$.

Transformer Decoder. The decoder in the transformer has a similar structure to the encoder, consisting of three stacked layers, each in turn consisting of three sublayers. A masked multi-head self-attention

sublayer is applied at the beginning, a feed-forward sublayer at the end of each layer and another multi-head *cross-attention* sublayer in the middle (Figure 3).

The inference process in the transformer decoder is auto-regressive, the model generates one token at a time and feeds it back as input for generating the next token, i.e. schedule position. As shown in Figure 4, in the first decoding step, the input to the decoder is the encoder output Z along with \Rightarrow indicating the beginning of a schedule. In the subsequent decoding steps, the decoder takes as input the output of the encoder along with the previously generated elements $(s_0, s_1, \dots, s_{i-1})$ to create an output $o_i \in \mathbb{R}^d$, encapsulating knowledge of the previously generated schedule elements up to the current decoding step and the contextual information provided by the encoder.

In the first sub-layer of the decoder, the masked multi-head attention uses the embedding of the last generated token s_{i-1} as the query, while the keys and values are the embeddings of the previously generated tokens $(s_0, s_1, \dots, s_{i-1})$. The mask ensures that the model does not attend to any tokens beyond the current position, preserving the autoregressive nature of the transformer. In the subsequent cross-attention sub-layer, the query is the output of the masked multi-head attention layer, while the keys and values are the encoder output Z . This allows the decoder to use the information from the input sequence while generating the output.

The total number of parameters per decoder layer is given by the number of parameters of the two multi-head self-attention sublayers ($2 \times 16,640$), feed-forward sublayer ($8,320$), and three layer normalization (3×128), which equals 41,984. For $N = 2$ decoder layers, the total number of parameters is equal to $2 \times 41,984 = 83,968$. In a traditional transformer network, the decoder output o_i is passed through a linear transformation followed by a softmax to generate a probability distribution over the target output space. In this study, however, we pass o_i to a *pointer attention* layer, as detailed below.

3.2.3 Pointer Attention Layer

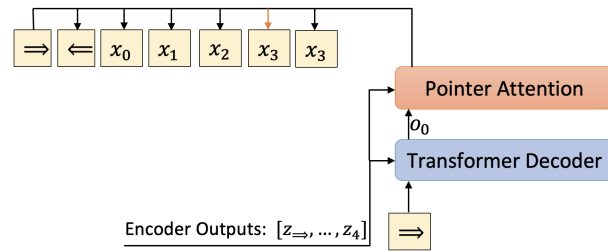
We obtained only a 45% validation accuracy using the traditional transformer. To address this challenge, we replaced the final linear layer in the transformer architecture with a pointer layer. The pointer layer uses attention to selectively point back to elements in the input set at each decoding step, allowing the model to dynamically focus on the most relevant elements. This is accomplished by combining the encoder output matrix Z and the decoder output vector o_i at decoding step i into attention weights u_j^i that represent the importance of each element j in the input with respect to the current decoding step o_i . The pointer attention score u_j^i is computed as:

$$u_j^i = \begin{cases} v^T \tanh(W_1 z_j^T + W_2 o_i^T) & \text{if } j \notin \{s_0, \dots, s_{i-1}\} \\ -\infty & \text{otherwise,} \end{cases}$$

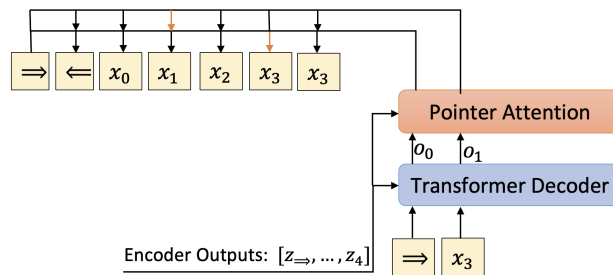
where $v \in \mathbb{R}^d$, $W_1 \in \mathbb{R}^{d \times d}$, and $W_2 \in \mathbb{R}^{d \times d}$ are learnable parameters of the model, represented as linear layers. The tanh activation function captures the non-linear relationship between the encoder output z_j for input token j and the decoder output o_i . To obtain the probability distribution $p(s_i | s_1, \dots, s_{i-1}, X)$, indicating the likelihood of selecting element s_i given the previous selections s_1, \dots, s_{i-1} and the input X , the softmax function is applied to the attention vector u^i , i.e. $p(s_i | s_1, \dots, s_{i-1}, X) = \text{softmax}(u^i)$.

The softmax function normalizes the vector u^i to create an output distribution over the input set. By setting the logits (log-probabilities) of input elements that have already appeared in the schedule to $-\infty$, we guarantee that the model only focuses on elements that have not yet been generated, preventing duplicate

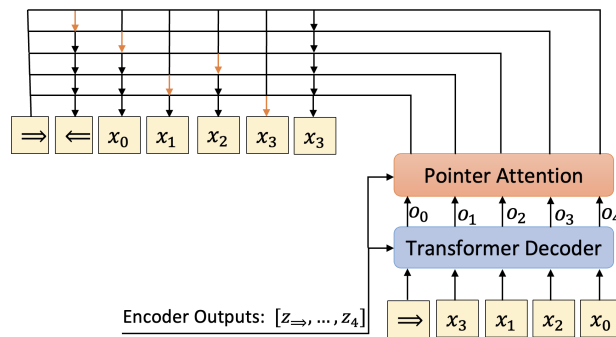
Figure 4: Autoregressive Inference of the Decoder. In the first step, the decoder takes as input the \Rightarrow and the encoder output matrix Z , producing o_0 . The pointer layer then uses o_0 and Z to select x_3 , as shown by the orange arrow. In the subsequent steps, the previously generated tokens are passed to the decoder and excluded from further selection in the pointer attention layer.



(a) First Decoding Step



(b) Second Decoding Step



(c) Last Decoding Step

selections. The pointer network learnable matrices are $W_1 \in R^{64 \times 64}$, $W_2 \in R^{64 \times 64}$, and vector $v \in R^{64}$. Thus, the number of learnable parameters for the pointer network is $2 \times 64 \times 64 + 64 = 8,256$. The total learnable parameters in the transformer-pointer architecture is given by the number of embedding, encoder, decoder, and pointer weights, for a total of $320 + 50,432 + 83,968 + 8,256 = 142,976$ learnable parameters.

4 Data Generation

To generate the dataset for training and validation, the column generation algorithm is executed by solving the pricing subproblems using dynamic programming. We generate instances with different number of jobs $N \in \{20, 30, 40, 60, 80\}$ and machines $M \in \{2, 4, 8, 12, 16\}$. In the first set of experiments, the job weights w_j and processing times p_{jk} are generated following [Chen and Powell \(1999\)](#), with integer weights uniformly drawn from $[1, 100]$ and integer processing times uniformly sampled from $[1, 30]$.

The testing data include instances generated using the same uniform distributions as well as out-of-distribution (OOD) instances in which the weights are independent integers drawn from a Weibull distribution with shape parameter $k = 1.5$ and scale parameter $\lambda = 50$, while the processing times are integers independently sampled from a Weibull distribution with shape parameter $k = 2$ and scale parameter $\lambda = 15$. We refer to the combination of the number of machines and the number of jobs as a problem class (for example, 2 machines and 20 jobs) and generate multiple instances from each class. We start the column generation with a specific number (5, 10, 20, 50, or 100) of initial columns per machine.

In each iteration of the column generation, the processing times and weights remain constant, but we obtain new dual values for jobs and machines. Using these updated dual values, we solve each subproblem using dynamic programming to generate a new negative reduced cost column per machine which serves as the target output s of the neural network. If a subproblem finds no negative reduced cost column, it returns an empty vector. Hence, after each CG iteration, we obtain one new data instance per machine.

We generate 73,144 data instances, of which 80% are used for training and 20% for validation. [Table 3](#) in [Appendix A](#) lists the percentage of training instances (data points) per problem class. Most problem classes have similar percentages except for those involving 2 machines and 20 jobs, and those with 4 machines and 60 jobs, which have the highest percentage of data points. The difference arises because it is difficult to control the exact number of subproblems that will be solved in the course of a given CG run. Although the data are not evenly distributed across the different problem classes, our results demonstrate that our model can effectively generalize to problems of varying sizes.

5 Computational Experiments

This section provides an overview of the training procedure, hyperparameter tuning, and the comparison of testing instances with the traditional column generation approach employing the dynamic programming procedure with the greedy selection of the most negative reduced-cost column. The entire implementation is done in Python. The restricted master problem is solved using Gurobi 9.1.2, while the training and testing of the neural network are conducted using PyTorch 1.13.1. We run the hyperparameter tuning and training on two Nvidia A100 GPUs. The testing and data generation are executed on an Apple M2 Pro.

5.1 Training

During the training process, we employ the teacher-forcing strategy (Williams and Zipser, 1989), which involves passing the previous steps of the target job sequence to the next decoding step, rather than using the model’s predicted output. For instance, in the second decoding step in Figure 4, the true target job in the first position is x_3 . Therefore, the input to the decoder in the second decoding step is \Rightarrow and x_3 regardless of the model’s prediction for the first position, which might not be x_3 .

We train the model using a negative log-likelihood loss function $l(\theta)$ measuring the cross-entropy between the predicted probabilities and the target schedule generated by the DP. Specifically,

$$l(\theta) = - \sum_{i=1}^n \log p(s_i|X; \theta),$$

where s_i is the target element in schedule position i . We employ the Adam optimizer (Kingman and Ba, 2015) with parameter values found through hyperparameter tuning. We assess the prediction performance using accuracy, which is calculated as the percentage of correctly predicted sequence positions.

5.2 Hyperparameter Tuning

Hyperparameter tuning is a crucial step in optimizing the performance of a neural network model. Table 1 includes the list of parameters along with their tested and the best-found values. The tested values for each parameter are chosen from the literature, and descriptions of these hyperparameters are given in Appendix B. To find the best configuration of these hyperparameters, we use RayTune (Liaw et al., 2018), a Python library that offers state-of-the-art tuning algorithms with the advantage of parallel computing. We use the Asynchronous Successive Halving Algorithm (Li et al., 2020), which combines random search with principled early stopping. This algorithm samples different combinations of hyperparameter values given in Table 1, and trains models in parallel. We conduct 100 trials, that is, sample 100 hyper parameter configurations (see Table 4 in Appendix B). Each trial involves training the model for 150 epochs. A complete pass through the training dataset is made during each epoch. The validation accuracy is used to evaluate the prediction performance, and a grace period of 5 epochs is set for early stopping. If the accuracy does not improve within the grace period, the trial is terminated early.

The results of the hyperparameter tuning, including the validation loss and accuracy over 150 training epochs, are presented in Figures 8 and 9, respectively, in Appendix B. Early stopped trials are represented by lines that terminate before reaching the maximum number of epochs. These trials exhibit a plateau in the validation loss, indicating that further training is unlikely to yield better results. After analyzing the initial 100 trials, we conducted an additional round of hyperparameter tuning that explored various key hyperparameters, including larger model dimensions (128 and 256), reduced weight decay ($1e-07$), an increased number of heads (16), larger batch sizes (64 and 128), and lower dropout rates. However, none outperformed the best configuration from the initial tuning.

6 Results

6.1 Training and Validation Results

The training and validation loss and accuracy for the best-found model are shown in Figure 5. The training loss demonstrates a decreasing trend, indicating that the model is effectively learning. The validation loss curve shows a decreasing trend, indicating the model’s ability to generalize to unseen data. The fact that

Table 1: Tested Values of the Hyperparameters and the Best Configuration

Hyperparameter	Tested Values	Best Found
Model Dimension	16, 32, 64	64
Number of Attention Heads	2, 4, 8	8
Number of Encoder Layers	1, 2, 3, 6	2
Number of Decoder Layers	1, 2, 3, 6	2
Dropout	0.0, 0.3, 0.5, 0.8	0.0
Weight Decay	0, 0.1, 0.01, 1e-3, 1e-5, 1e-6	1e-6
Batch Size	16, 32	16
Learning Rate	1e-5, 1e-4, 1e-3, 1e-2	1e-4

the validation loss is similar to the training loss suggests that the model is not overfitting. The validation accuracy reaches 86%, indicating that on average the model correctly predicts 86% of the positions in the target schedules in the unseen validation data.

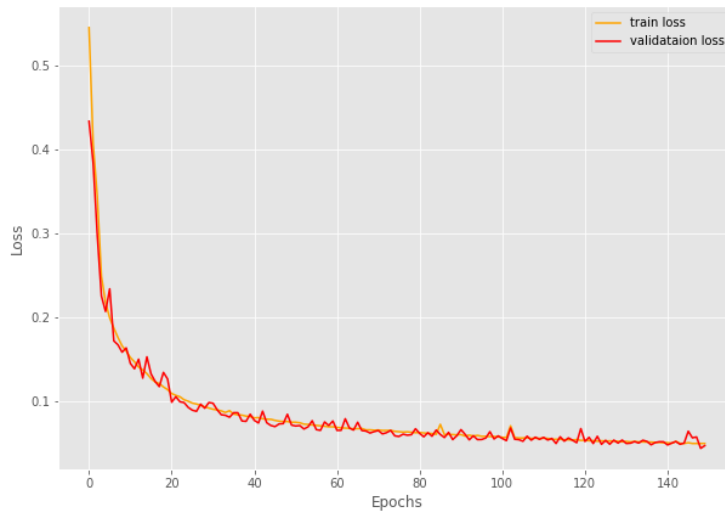
6.2 Testing Results

We conduct experiments to investigate the performance of the proposed method compared to that using dynamic programming to solve the pricing subproblems. We apply the SWPT order rule to the NN schedules minimizing the total completion time on the machine. The first set of experiments involves small to medium size problem instances, as shown in Table 2. Instance name (e.g. 2M20N_1_20) indicates the number of machines (2), number of jobs (20), seed number (1), and the number of initial columns per machine (20). We solve these instances to optimality using the baseline (traditional column generation (CG) with greedy dynamic programming) and the proposed approach. The table shows the total time required to reach optimality and the total number of generated columns for both approaches. The proposed approach achieves a significant time reduction as the instance size increases and generally adds more columns than the baseline approach. Interestingly, CG NN-DP produces fewer columns than CG-Greedy-DP in some smaller instances, such as 4M20N_1_10, 4M20N_3_10, 4M20N_4_10, and 4M30N_2_10; number of columns is shown in red in the table when NN generates fewer columns than DP.

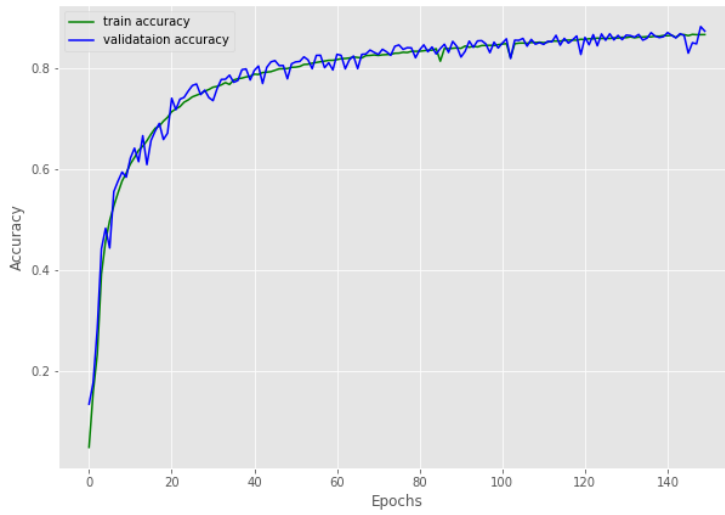
To show the performance of the proposed approach on large-scale instances, we compare it to multiple versions of column generation with DP. Specifically, we implement the CG-Greedy-DP, CG-DP-5, which adds the 5 most negative reduced columns per subproblem at each iteration, and CG-DP-20, which adds the 20 most negative reduced columns per subproblem at each iteration. Figure 6 shows the convergence plots for large-scale test instances with 8 machine 60 jobs, 16 machines 80 jobs, and 20 machines 100 jobs. We run 10 instances from each size for one hour, record the objective values of the RMP at each CG iteration and normalize them to be between $[0, 1]$ before taking the average over all instances of a given problem class. CG-NN-DP consistently outperforms other methods. Furthermore, as seen in Figure 6a, CG-NN-DP significantly improves the objective value within 100 seconds. As the instance size grows, the CG-DP approaches struggle to improve the objective value even after 3,600 seconds compared to a rapid improvement by CG-NN-DP as shown in the convergence plot of test instances with 20 machines and 100 jobs even though CG-NN-DP adds a single column per subproblem at each iteration. Figure 6c shows that CG-NN-DP performs very well for instances with 20 machines and 100 jobs, beyond the maximum training size of 80 jobs, demonstrating the generalizability of the proposed approach.

We also test the trained neural network on instances generated from Weibull distribution to evaluate the generalizability of the CG-NN-DP method to a class of instances different from the training set consisting

Figure 5: Training and Validation Loss and Accuracy

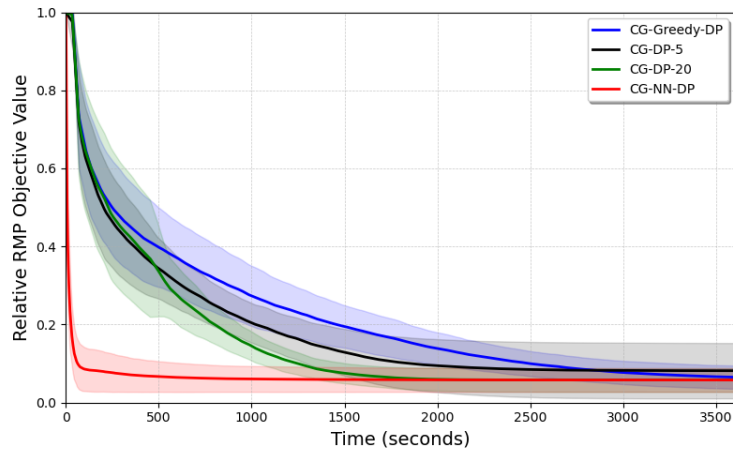


(a) Training and validation loss

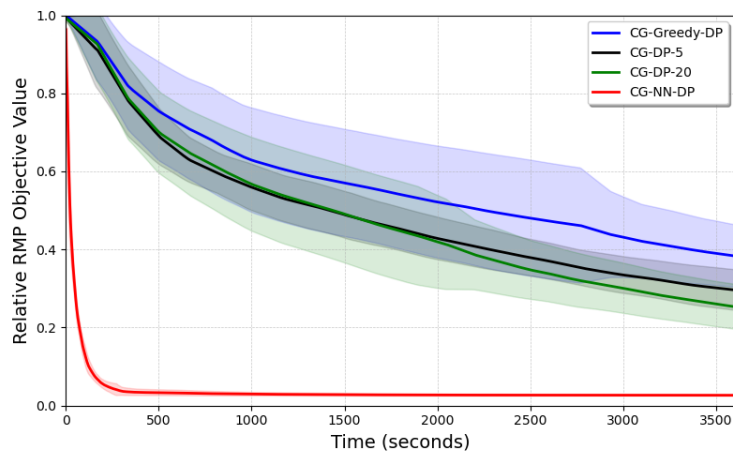


(b) Training and validation accuracy

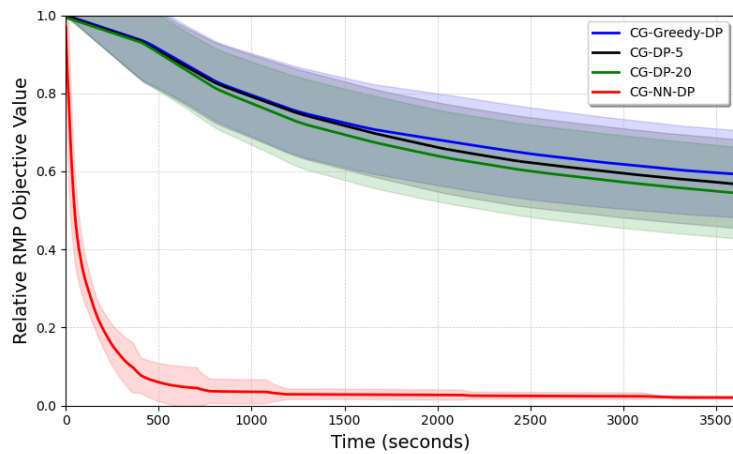
Figure 6: Convergence plots of different CG-DP approaches and CG-NN-DP for test instances 8M60N, 16M80N, and 20M100N generated from Uniform distribution. The solid curves are the mean of the relative objective values over 10 instances and the shaded area shows ± 1 standard deviation.



(a) 8 Machines 60 Jobs (8M60N)



(b) 16 Machines 80 Jobs (16M80N)



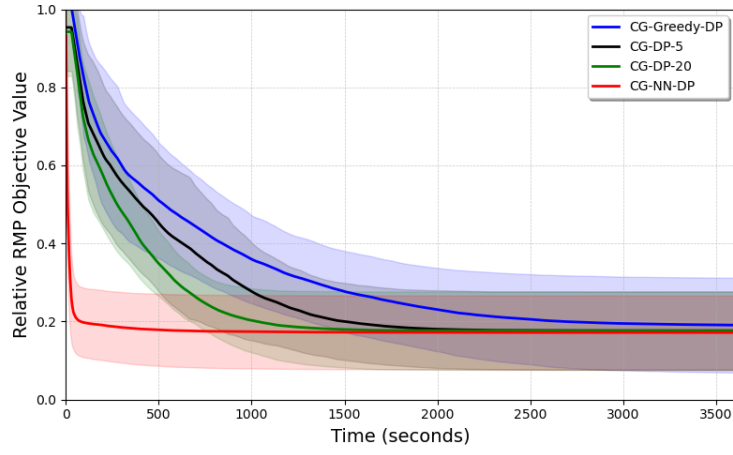
(c) 20 Machines 100 Jobs (20M100N)

Table 2: Computational Results for Small and Medium Size Instances

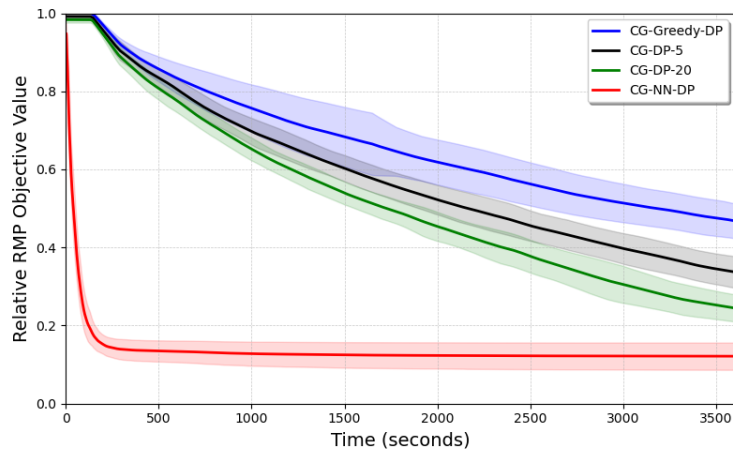
Instance	Total Time (sec)			Number of Columns Generated			
	CG-Greedy-DP	CG NN-DP	Time	CG-Greedy-DP	CG NN-DP		
			Reduction		Total	NN	DP
2M20N_1_20	45	30	33%	217	235	129	106
2M20N_2_20	39	20	49%	182	181	112	69
2M20N_3_20	34	29	14%	193	244	133	111
2M20N_4_20	31	13	58%	175	170	135	35
2M20N_5_20	39	26	33%	204	241	144	97
2M20N_6_10	35	20	43%	200	237	162	75
2M20N_7_10	32	18	42%	194	206	133	73
2M20N_8_10	36	20	44%	215	210	125	85
2M20N_9_10	46	35	24%	214	219	99	120
2M20N_10_10	44	24	45%	212	242	151	91
Average	38.1	23.5	38.5%	200.6	218.5	132.2	86.2
4M20N_1_10	45	30	33%	215	180	84	96
4M20N_2_10	35	20	43%	184	185	115	70
4M20N_3_10	31	20	35%	176	172	97	75
4M20N_4_10	37	11	70%	192	159	125	34
4M20N_5_10	42	22	48%	215	209	153	56
4M20N_6_5	36	22	37%	198	200	121	79
4M20N_7_5	40	19	52%	218	218	158	60
4M20N_8_5	38	17	55%	222	217	153	64
4M20N_9_5	53	29	45%	256	231	123	108
4M20N_10_5	45	25	44%	217	202	109	93
Average	40.2	21.5	46.2%	209.3	197.3	123.8	73.5
2M30N_1_20	309	151	51%	462	551	376	175
2M30N_2_20	336	96	71%	501	556	444	112
2M30N_3_20	267	153	43%	499	631	417	214
2M30N_4_20	248	152	39%	420	598	391	207
2M30N_5_20	347	139	60%	575	590	408	182
2M30N_6_10	270	164	39%	466	632	387	245
2M30N_7_10	327	143	56%	558	623	434	189
2M30N_8_10	242	121	50%	495	558	369	189
2M30N_9_10	336	165	51%	526	622	404	218
2M30N_10_10	308	170	45%	486	625	386	239
Average	299	145.4	50.5%	498.8	598.6	401.6	197
4M30N_1_10	294	157	46%	457	466	269	197
4M30N_2_10	355	173	51%	511	455	321	134
4M30N_3_10	237	87	63%	430	392	295	97
4M30N_4_10	298	155	48%	491	512	361	151
4M30N_5_10	330	172	47%	507	503	311	192
4M30N_6_5	265	123	53%	476	470	332	138
4M30N_7_5	237	135	43%	421	512	351	161
4M30N_8_5	266	80	70%	498	439	325	114
4M30N_9_5	303	126	58%	514	528	357	171
4M30N_10_5	352	94	73%	517	461	355	106
Average	287.2	134.2	53.2%	478.3	475.2	324.7	150.6
2M40N_1_20	1929	1140	41%	1117	1364	639	725

of instances generated from Uniform distribution. The results in Figure 7 again demonstrates the superior performance of CG-NN-DP compared to the other CG-DP approaches considered.

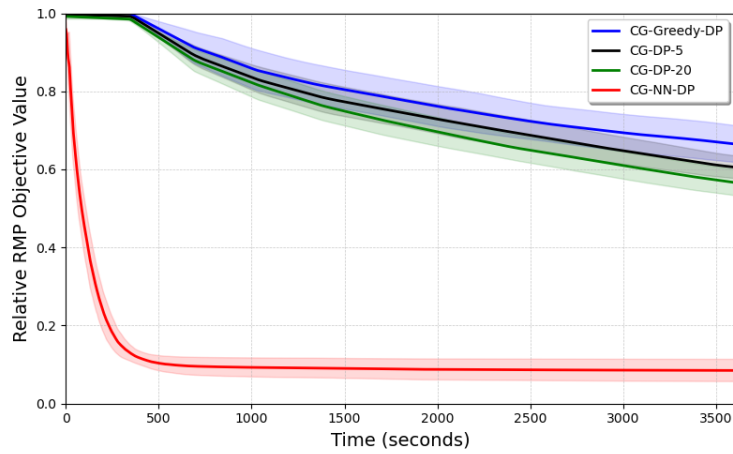
Figure 7: Convergence plots of different CG-DP approaches and CG-NN-DP for test instances 8M60N, 16M80N, and 20M100N generated from Weibull distribution. The solid curves are the mean of the relative objective values over 10 instances and the shaded area shows ± 1 standard deviation.



(a) 8 Machines 60 Jobs (8M60N)



(b) 16 Machines 80 Jobs (16M80N)



(c) 20 Machines 100 Jobs (20M100N)

7 Conclusion and Future Research Directions

In this paper, we train a transformer pointer network to rapidly approximate the dynamic programming solution of the pricing subproblem for minimizing the total weighted completion time on unrelated parallel machines. Our approach achieves significantly faster convergence than the traditional CG with dynamic programming, and exhibits generalization capability beyond the maximum number of jobs considered during training as well as to out-of-distribution instances.

An interesting future direction is exploring the application of transfer learning (Torrey and Shavlik, 2010) to extend the proposed NN architecture to other scheduling problems. By leveraging the knowledge gained from solving the total weighted completion time problem on unrelated parallel machines, transfer learning could enable faster adaptation of the proposed neural network architecture to parallel machine scheduling problems with different performance measures. This approach has the potential to significantly reduce the need for extensive retraining on new problem instances, improving efficiency across a broader range of scheduling problems.

In this work, the NN adds a single column per machine at each iteration of the column generation process. As a future direction, we plan to explore the possibility of extending the approach to add multiple columns using beam search decoding (Vijayakumar et al., 2016) instead of greedy decoding. Beam search can generate multiple schedules (job sequences) by sampling various candidate jobs at each decoding step, rather than selecting only the schedule with the highest likelihood. By introducing this enhancement, we anticipate further improvements in the efficiency and effectiveness of the proposed CG-NN-DP approach.

Our supervised learning approach to training the transformer pointer network is susceptible to exposure bias (Bengio et al., 2015). To address this issue, we intend to investigate the application of reinforcement learning and self-supervised learning as alternative training methods. Both of these approaches would allow the neural network to learn based on the reduced costs of generated columns without relying on labeled data, but they follow distinct strategies. Reinforcement learning involves training the network in an environment and requires extensive exploration and the optimization of a reward function (Wiering and Van Otterlo, 2012). In contrast, self-supervised learning requires large amounts of unlabeled data to learn inherent patterns in the problem structure (Cai et al., 2024).

Finally, it is worth considering the direct application of neural networks to the original parallel machine scheduling problem without relying on column generation. A neural network-based optimization proxy could be trained to approximate the solution to the original scheduling problem, potentially eliminating the need for the CG framework. This approach, however, might be more data-intensive and computationally demanding, especially for large instances.

8 Acknowledgements

This research was supported by the National Science Foundation (NSF) under Grant CMMI-1826125. Any opinions stated are those of the authors, and do not necessarily reflect those of NSF.

References

- Azizoglu, M., Kirca, O., 1999. Scheduling jobs on unrelated parallel machines to minimize regular total cost functions. *IIE transactions* 31, 153–159.
- Ba, J.L., Kiros, J.R., Hinton, G.E., 2016. Layer normalization. *arXiv preprint arXiv:1607.06450*.
- Baesler, F., Palma, C., 2014. Multiobjective parallel machine scheduling in the sawmill industry using memetic algorithms. *The International Journal of Advanced Manufacturing Technology* 74, 757–768.
- Bengio, S., Vinyals, O., Jaitly, N., Shazeer, N., 2015. Scheduled sampling for sequence prediction with recurrent neural networks. *Advances in neural information processing systems* 28.
- Bengio, Y., Lodi, A., Prouvost, A., 2021. Machine learning for combinatorial optimization: a methodological tour d’horizon. *European Journal of Operational Research* 290, 405–421.
- Bresson, X., Laurent, T., 2021. The transformer network for the traveling salesman problem. *arXiv preprint arXiv:2103.03012*.
- Cai, Q., Guo, X., Huang, S., 2024. A self-supervised learning model for graph clustering optimization problems. *Knowledge-Based Systems* 290, 111549.
- Cappart, Q., Chételat, D., Khalil, E.B., Lodi, A., Morris, C., Veličković, P., 2023. Combinatorial optimization and reasoning with graph neural networks. *Journal of Machine Learning Research* 24, 1–61.
- Chen, Z.L., Powell, W.B., 1999. Solving parallel machine scheduling problems by column generation. *INFORMS Journal on Computing* 11, 78–94.
- Chi, C., Aboussalah, A.M., Khalil, E.B., Wang, J., Sherkat-Masoumi, Z., 2022. A deep reinforcement learning framework for column generation. *arXiv preprint arXiv:2206.02568*.
- Dantzig, G.B., Wolfe, P., 1960. Decomposition principle for linear programs. *Operations Research* 8, 101–111.
- Durasević, M., Jakobović, D., 2023. Heuristic and metaheuristic methods for the parallel unrelated machines scheduling problem: a survey. *Artificial Intelligence Review* 56, 3181–3289.
- Fan, Z., Ghaddar, B., Wang, X., Xing, L., Zhang, Y., Zhou, Z., 2024. Artificial intelligence for operations research: Revolutionizing the operations research process. *arXiv preprint arXiv:2401.03244*.
- Garey, M.R., Johnson, D.S., 1979. *Computers and intractability*. volume 174. W. H. Freeman, San Francisco.
- Hall, N.G., Potts, C.N., Sriskandarajah, C., 2000. Parallel machine scheduling with a common server. *Discrete Applied Mathematics* 102, 223–243.
- Hertrich, C., Skutella, M., 2023. Provably good solutions to the knapsack problem via neural networks of bounded size. *INFORMS journal on computing* 35, 1079–1097.
- Khalil, E., Le Bodic, P., Song, L., Nemhauser, G., Dilkina, B., 2016. Learning to branch in mixed integer programming, in: *Proceedings of the AAAI conference on artificial intelligence*.
- Kingma, D.P., Ba, J., 2014. Adam: A method for stochastic optimization. *arXiv preprint arXiv:1412.6980*.

- Kingman, D., Ba, J., 2015. Adam: A method for stochastic optimization., in: 3rd International Conference for Learning Representations.
- Kool, W., Van Hoof, H., Welling, M., 2018. Attention, learn to solve routing problems! arXiv preprint arXiv:1803.08475.
- Kotary, J., Fioretto, F., Van Hentenryck, P., Wilder, B., 2021. End-to-end constrained optimization learning: A survey. arXiv preprint arXiv:2103.16378.
- Lawler, E.L., Lenstra, J.K., Kan, A.H.R., Shmoys, D.B., 1993. Sequencing and scheduling: Algorithms and complexity. *Handbooks in Operations Research and Management Science* 4, 445–522.
- Lee, J., Kee, S., Janakiram, M., Runger, G., 2024. Attention-based reinforcement learning for combinatorial optimization: Application to job shop scheduling problem. arXiv preprint arXiv:2401.16580.
- Li, K., Yang, S.L., 2009. Non-identical parallel-machine scheduling research with minimizing total weighted completion times: Models, relaxations and algorithms. *Applied Mathematical Modelling* 33, 2145–2158.
- Li, L., Jamieson, K., Rostamizadeh, A., Gonina, E., Ben-Tzur, J., Hardt, M., Recht, B., Talwalkar, A., 2020. A system for massively parallel hyperparameter tuning. *Proceedings of Machine Learning and Systems* 2, 230–246.
- Liaw, R., Liang, E., Nishihara, R., Moritz, P., Gonzalez, J.E., Stoica, I., 2018. Tune: A research platform for distributed model selection and training. arXiv preprint arXiv:1807.05118.
- Lübbecke, M.E., Desrosiers, J., 2005. Selected topics in column generation. *Operations Research* 53, 1007–1023.
- Ma, Q., Ge, S., He, D., Thaker, D., Drori, I., 2019. Combinatorial optimization by graph pointer networks and hierarchical reinforcement learning. arXiv preprint arXiv:1911.04936.
- Mazyavkina, N., Sviridov, S., Ivanov, S., Burnaev, E., 2021. Reinforcement learning for combinatorial optimization: A survey. *Computers & Operations Research* 134, 105400.
- Mokotoff, E., 2001. Parallel machine scheduling problems: A survey. *Asia-Pacific Journal of Operational Research* 18, 193.
- Morabit, M., Desaulniers, G., Lodi, A., 2021. Machine-learning-based column selection for column generation. *Transportation Science* 55, 815–831.
- Ojha, R., Chen, W., Zhang, H., Khir, R., Erera, A., Van Hentenryck, P., 2023. Optimization-based learning for dynamic load planning in trucking service networks. arXiv preprint arXiv:2307.04050.
- Pfund, M., Fowler, J.W., Gupta, J.N., 2004. A survey of algorithms for single and multi-objective unrelated parallel-machine deterministic scheduling problems. *Journal of the Chinese Institute of Industrial Engineers* 21, 230–241.
- Phillips, C., Stein, C., Wein, J., 1994. Task scheduling in networks, in: *Scandinavian Workshop on Algorithm Theory*, Springer. 290–301.
- Pinedo, M., 2012. *Scheduling: Theory, Algorithms and Systems*. volume 29. Springer.

- Rajabalizadeh, A., Davarnia, D., 2024. Solving a class of cut-generating linear programs via machine learning. *INFORMS Journal on Computing*.
- Rothkopf, M.H., 1966. Scheduling independent tasks on parallel processors. *Management Science* 12, 437–447.
- Shen, Y., Sun, Y., Li, X., Eberhard, A., Ernst, A., 2022. Enhancing column generation by a machine-learning-based pricing heuristic for graph coloring, in: *Proceedings of the AAAI Conference on Artificial Intelligence*, 9926–9934.
- Smith, W.E., et al., 1956. Various optimizers for single-stage production. *Naval Research Logistics Quarterly* 3, 59–66.
- Srivastava, N., Hinton, G., Krizhevsky, A., Sutskever, I., Salakhutdinov, R., 2014. Dropout: a simple way to prevent neural networks from overfitting. *The journal of machine learning research* 15, 1929–1958.
- Stohy, A., Abdelhakam, H.T., Ali, S., Elhenawy, M., Hassan, A.A., Masoud, M., Glaser, S., Rakotonirainy, A., 2021. Hybrid pointer networks for traveling salesman problems optimization. *Plos one* 16, e0260995.
- Sugishita, N., Grothey, A., McKinnon, K., 2024. Use of machine learning models to warmstart column generation for unit commitment. *INFORMS Journal on Computing*.
- Sutskever, I., Vinyals, O., Le, Q.V., 2014. Sequence to sequence learning with neural networks. *Advances in Neural Information Processing Systems* 27.
- Tang, Y., Agrawal, S., Faenza, Y., 2020. Reinforcement learning for integer programming: Learning to cut, in: *International Conference on Machine Learning*, PMLR. 9367–9376.
- Torrey, L., Shavlik, J., 2010. Transfer learning, in: *Handbook of research on machine learning applications and trends: algorithms, methods, and techniques*. IGI global, 242–264.
- Vaswani, A., Shazeer, N., Parmar, N., Uszkoreit, J., Jones, L., Gomez, A.N., Kaiser, L., Polosukhin, I., 2017. Attention is all you need. *arXiv preprint arXiv:1706.03762*.
- Vijayakumar, A.K., Cogswell, M., Selvaraju, R.R., Sun, Q., Lee, S., Crandall, D., Batra, D., 2016. Diverse beam search: Decoding diverse solutions from neural sequence models. *arXiv preprint arXiv:1610.02424*.
- Vinyals, O., Fortunato, M., Jaitly, N., 2015. Pointer networks. *Advances in neural information processing systems* 28.
- Wang, R., Zhou, Z., Li, K., Zhang, T., Wang, L., Xu, X., Liao, X., 2024. Learning to branch in combinatorial optimization with graph pointer networks. *IEEE/CAA Journal of Automatica Sinica* 11, 157–169.
- Weng, M.X., Lu, J., Ren, H., 2001. Unrelated parallel machine scheduling with setup consideration and a total weighted completion time objective. *International Journal of Production Economics* 70, 215–226.
- Wiering, M.A., Van Otterlo, M., 2012. Reinforcement learning. *Adaptation, Learning, and Optimization* 12, 729.
- Wilhelm, W.E., 2001. A technical review of column generation in integer programming. *Optimization and Engineering* 2, 159–200.

- Williams, R.J., Zipser, D., 1989. A learning algorithm for continually running fully recurrent neural networks. *Neural Computation* 1, 270–280.
- Wu, X., Wang, D., Wen, L., Xiao, Y., Wu, C., Wu, Y., Yu, C., Maskell, D.L., Zhou, Y., 2024. Neural combinatorial optimization algorithms for solving vehicle routing problems: A comprehensive survey with perspectives. arXiv preprint arXiv:2406.00415.
- Yalaoui, F., Chu, C., 2002. Parallel machine scheduling to minimize total tardiness. *International Journal of Production Economics* 76, 265–279.
- Yildiz, B., 2022. Reinforcement learning using fully connected, attention, and transformer models in knapsack problem solving. *Concurrency and Computation: Practice and Experience* 34, e6509.
- Yun, S., Jeong, M., Kim, R., Kang, J., Kim, H.J., 2020. Graph transformer networks.
- Zhang, J., Liu, C., Li, X., Zhen, H.L., Yuan, M., Li, Y., Yan, J., 2023. A survey for solving mixed integer programming via machine learning. *Neurocomputing* 519, 205–217.

A Data points generated from each problem class

Table 3: Data points generated from each problem class.

Machines (M)	Jobs (N)	Percentage of data points	Number of data points
2	20	17.20%	12,576
2	30	2.30%	1,660
2	40	5.90%	4,308
4	20	3.50%	2,556
4	30	1.90%	1,384
4	40	5.90%	4,296
4	60	13.20%	9,664
8	20	0.40%	296
8	40	5.10%	3,736
8	60	6.90%	5,024
8	80	7.20%	5,232
12	40	5.70%	4,200
12	60	6.00%	4,440
12	80	4.10%	2,964
16	40	2.60%	1,920
16	60	5.60%	4,128
20	60	6.50%	4,760

B Hyperparameter Tuning

The considered hyperparameters are:

1. Model dimension (d): Determines the embedding dimension of the model and the size of the subsequent layers after the embedding layer.
2. Number of attention heads (h): In the multi-head attention sublayers, the input is split into multiple heads, with each attending to different parts of the input. The number of heads determines the level of parallelization and the model’s ability to capture different types of interconnections between elements.
3. Number of encoder and decoder layers: Defines the number of layers in the encoder of layers allows the model to capture more complex features but increases computational cost.
4. Dropout rate: A regularization technique that randomly deactivates a certain percentage of neurons during training, reducing the model’s reliance on specific connections and preventing overfitting (Srivastava et al., 2014).
5. L_2 weight decay: Adds a penalty term to the loss function based on the magnitude of the weights to prevent overfitting by encouraging smaller weights and reduce model complexity.
6. Batch size: The number of training examples processed together in each iteration of the training procedure. Larger batch sizes can provide a smoother gradient estimate but require more memory and computational resources.
7. Learning rate: The learning rate, denoted by α in the Adam optimizer (Kingma and Ba, 2014), controls the step size during gradient descent optimization. It determines how quickly the model updates its

parameters based on the gradients. Choosing an appropriate learning rate is crucial for achieving good convergence during training.

We report the results of 100 hyperparameter configurations and their associated validation loss and accuracy in Table 4. Figures 9 and 8 show the results of the hyperparameter tuning trials, including the validation loss and accuracy over 150 training epochs. Early stopped trials are represented by lines that terminate before reaching the maximum number of epochs. These trials exhibit a plateau in the validation loss, suggesting further training is unlikely to improve results.

Table 4: Evaluated Hyperparameter Tuning Configurations and Validation Accuracy

Trial	Hyperparameter Config	Loss	Accuracy %
1	(32, 4, 6, 6, 0.8, 0.001, 32, 0.0001)	0.57	17.96
2	(32, 8, 3, 3, 0.8, 0.001, 16, 0.001)	0.26	39.68
3	(64, 4, 3, 6, 0.0, 0.1, 16, 0.001)	0.93	0
4	(16, 4, 2, 3, 0.3, 0.001, 16, 1e-05)	0.66	0
5	(64, 8, 3, 2, 0.5, 1e-05, 16, 1e-05)	0.57	7.39
6	(64, 2, 3, 6, 0.0, 0.1, 32, 0.01)	3.98	0
7	(32, 4, 3, 3, 0.5, 0.1, 16, 1e-05)	0.76	0
8	(32, 2, 2, 1, 0.3, 0.1, 32, 0.01)	1.17	0.55
9	(64, 4, 2, 2, 0.0, 1e-05, 32, 0.0001)	0.09	79.39
10	(16, 8, 1, 1, 0.8, 1e-05, 16, 0.0001)	0.58	5.29
11	(32, 2, 6, 3, 0.5, 0.1, 16, 0.01)	3.98	0
12	(16, 8, 3, 6, 0.3, 0.0, 32, 0.01)	2.37	0
13	(32, 4, 3, 3, 0.0, 0.0, 32, 0.0001)	0.07	82.19
14	(64, 2, 3, 1, 0.8, 0.0, 32, 0.001)	1.57	5.14
15	(32, 8, 3, 3, 0.3, 0.1, 32, 0.0001)	0.66	0
16	(16, 8, 3, 2, 0.0, 1e-06, 32, 0.01)	2.27	0
17	(32, 2, 2, 1, 0.0, 0.01, 32, 1e-05)	0.63	0
18	(16, 2, 3, 1, 0.8, 0.0, 16, 0.01)	3.98	2.87
19	(16, 8, 3, 6, 0.0, 0.0, 16, 1e-05)	0.6	0
20	(32, 2, 6, 1, 0.8, 0.1, 32, 0.001)	0.64	0
21	(64, 4, 6, 1, 0.5, 0.0, 16, 0.01)	3.98	1.83
22	(32, 8, 1, 3, 0.3, 1e-06, 32, 0.01)	1.75	0
23	(32, 8, 2, 6, 0.5, 1e-06, 16, 0.01)	3.49	0.78
24	(64, 4, 1, 6, 0.5, 0.01, 16, 0.001)	0.94	0
25	(64, 4, 6, 1, 0.3, 1e-06, 32, 1e-05)	0.53	10.66
26	(64, 8, 2, 1, 0.3, 0.0, 16, 1e-05)	0.51	11.56
27	(32, 2, 6, 1, 0.5, 1e-06, 32, 0.001)	0.22	52.19
28	(16, 2, 2, 1, 0.8, 0.001, 32, 1e-05)	2.68	2.78
29	(64, 4, 3, 3, 0.0, 0.0, 32, 1e-05)	0.43	16.63
30	(32, 8, 3, 3, 0.5, 0.0, 32, 1e-05)	0.67	0
31	(16, 4, 2, 6, 0.0, 1e-06, 32, 0.0001)	0.11	73.06
32	(16, 2, 6, 6, 0.3, 0.001, 32, 1e-05)	1.12	0
33	(16, 4, 6, 2, 0.8, 0.1, 16, 0.001)	0.67	0

34	(16, 8, 3, 3, 0.0, 0.01, 16, 0.001)	0.91	0
35	(64, 4, 1, 2, 0.3, 0.1, 16, 0.0001)	0.63	0
36	(32, 4, 2, 6, 0.8, 1e-05, 16, 1e-05)	1.52	0
37	(16, 4, 1, 6, 0.0, 1e-05, 32, 1e-05)	0.84	0
38	(16, 4, 2, 6, 0.5, 0.01, 16, 0.01)	1.05	0
39	(64, 8, 6, 1, 0.5, 0.0, 16, 1e-05)	0.55	8.66
40	(32, 4, 2, 6, 0.5, 0.001, 32, 0.01)	4.05	1.93
41	(64, 4, 1, 3, 0.3, 0.0, 32, 0.0001)	0.24	43.48
42	(64, 2, 3, 3, 0.5, 0.001, 16, 0.01)	3.98	1.87
43	(16, 4, 3, 1, 0.0, 0.1, 16, 0.0001)	0.6	0
44	(32, 4, 1, 6, 0.3, 0.1, 16, 0.0001)	0.65	0
45	(16, 2, 2, 3, 0.5, 1e-06, 16, 0.001)	0.19	57.55
46	(32, 8, 3, 1, 0.8, 0.0, 16, 1e-05)	2.11	0
47	(64, 8, 3, 2, 0.5, 0.001, 32, 0.0001)	0.33	24.74
48	(32, 8, 3, 6, 0.3, 0.01, 16, 0.0001)	0.42	17.9
49	(32, 2, 2, 3, 0.5, 0.1, 16, 0.01)	1.7	0.01
50	(16, 8, 3, 1, 0.0, 1e-06, 16, 1e-05)	0.58	0
51	(32, 2, 3, 3, 0.3, 1e-05, 32, 0.0001)	0.35	23.89
52	(16, 2, 1, 3, 0.8, 0.0, 16, 1e-05)	1.48	0.31
53	(32, 8, 3, 6, 0.3, 1e-05, 32, 0.01)	3.98	0
54	(16, 8, 2, 3, 0.0, 0.1, 16, 0.0001)	0.6	0
55	(16, 8, 3, 1, 0.0, 0.001, 16, 1e-05)	0.6	0
56	(16, 4, 2, 2, 0.8, 0.0, 16, 0.0001)	0.67	3.11
57	(64, 8, 6, 1, 0.3, 1e-05, 16, 0.0001)	0.07	82.6
58	(64, 8, 3, 3, 0.5, 0.1, 32, 0.01)	1.02	0
59	(64, 8, 2, 2, 0.0, 0.01, 16, 1e-05)	0.54	8.9
60	(16, 2, 1, 6, 0.3, 1e-05, 16, 0.001)	0.17	60.45
61	(64, 4, 2, 2, 0.5, 0.0, 32, 0.0001)	0.23	45.72
62	(32, 8, 6, 3, 0.5, 1e-06, 32, 1e-05)	0.65	0
63	(32, 8, 1, 2, 0.8, 1e-05, 32, 0.001)	0.23	48.1
64	(16, 8, 6, 1, 0.3, 1e-05, 16, 0.01)	3.98	1.88
65	(64, 2, 3, 3, 0.0, 1e-05, 32, 0.01)	2.21	0
66	(16, 4, 2, 1, 0.0, 0.0, 16, 0.0001)	0.11	74.69
67	(32, 8, 2, 6, 0.5, 1e-06, 32, 0.01)	4.06	0.21
68	(32, 2, 3, 3, 0.3, 0.1, 16, 1e-05)	0.72	0
69	(64, 4, 1, 3, 0.8, 1e-05, 16, 0.001)	0.52	18.46
70	(64, 2, 6, 3, 0.5, 0.001, 16, 0.001)	0.28	43.26
71	(32, 2, 6, 3, 0.5, 0.1, 16, 0.001)	1.05	0.01
72	(64, 2, 6, 3, 0.5, 1e-06, 32, 0.001)	0.19	56.68
73	(64, 4, 6, 2, 0.8, 0.001, 16, 0.01)	3.98	1.94
74	(64, 8, 2, 3, 0.3, 0.001, 32, 0.0001)	0.23	45.73
75	(64, 8, 2, 2, 0.0, 1e-06, 16, 0.0001)	0.06	85.71
76	(16, 8, 1, 2, 0.5, 0.001, 32, 0.001)	0.26	41.5
77	(16, 4, 2, 3, 0.0, 0.0, 32, 0.01)	2.16	0.21
78	(64, 2, 2, 3, 0.3, 0.01, 16, 1e-05)	0.59	0

79	(32, 2, 6, 3, 0.3, 0.01, 16, 0.0001)	0.57	5.13
80	(16, 2, 3, 3, 0.3, 0.001, 32, 1e-05)	0.94	0
81	(64, 2, 2, 6, 0.0, 1e-05, 16, 0.001)	0.91	0
82	(16, 4, 1, 6, 0.5, 0.1, 16, 0.01)	1.14	0.28
83	(32, 2, 3, 2, 0.0, 1e-05, 16, 1e-05)	0.44	15.98
84	(16, 8, 2, 3, 0.5, 0.01, 32, 0.001)	0.6	0
85	(16, 8, 1, 3, 0.8, 1e-05, 16, 0.01)	1.78	0
86	(32, 8, 3, 1, 0.3, 1e-06, 16, 0.0001)	0.13	70.14
87	(64, 8, 1, 3, 0.5, 0.01, 32, 0.0001)	0.59	0
88	(64, 4, 1, 2, 0.8, 0.0, 32, 0.01)	2.65	0.01
89	(16, 2, 1, 1, 0.3, 1e-05, 16, 0.0001)	0.57	0
90	(32, 2, 3, 1, 0.5, 1e-05, 32, 0.01)	3.98	5.22
91	(32, 4, 1, 1, 0.8, 0.01, 16, 0.0001)	0.61	0
92	(64, 4, 3, 6, 0.5, 0.001, 16, 0.01)	2.33	0.72
93	(32, 8, 2, 2, 0.3, 1e-05, 16, 0.001)	0.15	63.35
94	(64, 2, 2, 3, 0.5, 0.001, 32, 0.0001)	0.37	19.63
95	(64, 4, 1, 3, 0.5, 0.01, 32, 0.01)	1.38	0.73
96	(32, 2, 6, 6, 0.5, 0.01, 16, 1e-05)	0.63	0
97	(16, 2, 3, 2, 0.8, 0.001, 16, 0.01)	1.99	3.47
98	(32, 2, 1, 6, 0.0, 1e-06, 32, 0.0001)	0.15	64.16
99	(16, 8, 1, 6, 0.8, 1e-05, 16, 0.01)	3.36	0
100	(32, 4, 1, 3, 0.8, 0.01, 32, 1e-05)	1.92	0

Figure 8: Validation Loss Vs. Epoch. Each line corresponds to a hyperparameter configuration.

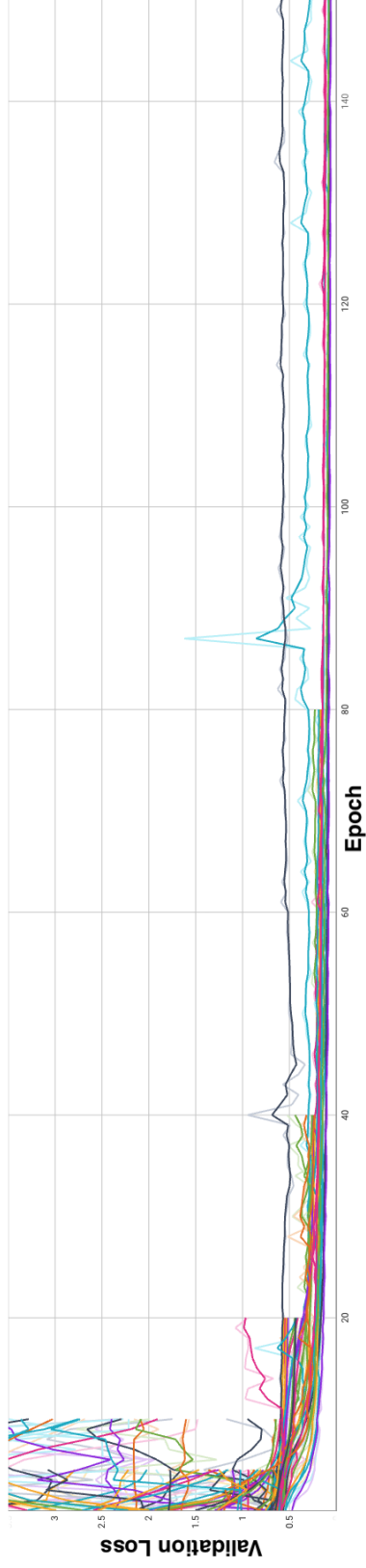


Figure 9: Validation Accuracy Vs. Epoch. Each line corresponds to a hyperparameter configuration.

